Hindawi Publishing Corporation
EURASIP Journal on Applied Signal Processing
Volume 2006, Article ID 49257, Pages 1–8
DOI 10.1155/ASP/2006/49257

Performance Analysis of the Blind Minimum Output Variance Estimator for Carrier Frequency Offset in OFDM Systems

Feng Yang, Kwok H. Li, and Kah C. Teh

School of Electrical and Electronic Engineering, Nanyang Technological University, Singapore 639798, Singapore

Received 18 November 2004; Revised 13 July 2005; Accepted 29 December 2005

Recommended for Publication by Alexei Gorokhov

Carrier frequency offset (CFO) is a serious drawback in orthogonal frequency division multiplexing (OFDM) systems. It must be estimated and compensated before demodulation to guarantee the system performance. In this paper, we examine the performance of a blind minimum output variance (MOV) estimator. Based on the derived probability density function (PDF) of the output magnitude, its mean and variance are obtained and it is observed that the variance reaches the minimum when there is no frequency offset. This observation motivates the development of the proposed MOV estimator. The theoretical mean-square error (MSE) of the MOV estimator over an AWGN channel is obtained. The analytical results are in good agreement with the simulation results. The performance evaluation of the MOV estimator is extended to a frequency-selective fading channel and the maximal-ratio combining (MRC) technique is applied to enhance the MOV estimator's performance. Simulation results show that the MRC technique significantly improves the accuracy of the MOV estimator.

1. INTRODUCTION

Orthogonal frequency division multiplexing (OFDM) has been considered as a promising modulation scheme for the next generation wireless communication systems. OFDM signals are transmitted in parallel subchannels, which are frequency-nonselective and overlapped in spectra. Hence, OFDM systems are robust to frequency-selective fading and enjoy high bandwidth efficiency. As the symbol duration is extended, the OFDM scheme reduces the normalized delay spread and avoids intersymbol interference (ISI). Because of these excellent characteristics, OFDM has been suggested and standardized for high-speed communications in Europe for digital audio broadcasting (DAB) [1] and terrestrial digital video broadcasting (DVB) [2]. Furthermore, OFDM is standardized for broadband wireless local area networks, for example, ETSI-BRAN High-performance local area networks (Hiperlan/2) [3], IEEE 802.11a [4], and for broadband wireless access, for example, IEEE 802.16 [5]. One drawback of OFDM systems is that carrier frequency offset (CFO) between the transmitter and receiver may degrade system performance severely [6]. CFO causes a number of impairments, including the attenuation and phase rotation of each of the subcarriers and intercarrier interference (ICI). Many estimation techniques have been proposed to estimate and correct the CFO before demodulation. Moose proposed a scheme to estimate CFO by repeating a data symbol and comparing the phase of each of the subcarriers between successive symbols [7]. However, this scheme adds more overhead and reduces the bandwidth efficiency. Schmidl and Cox proposed an estimation algorithm for timing offset and carrier frequency offset estimation based on the training sequence [8]. To improve the bandwidth efficiency, many blind estimation techniques have been proposed. van de Beek et al. developed a maximum-likelihood (ML) estimator by exploiting the redundancy in the cyclic prefix (CP) [9]. This method, however, suffers from performance degradation when the delay spread is comparable to the length of CP. Luise et al. exploited the time-frequency domain exchange inherent to the modulation scheme and proposed a blind algorithm for CFO recovery [10]. Tureli et al. utilized the shift invariant feature of the signal structure and extended ESPRIT algorithm to estimate CFO [11]. Tureli et al. exploited the inherent orthogonality between information-bearing carriers and virtual carriers, and proposed an algorithm to estimate the CFO [12]. Because of the presence of the virtual carriers for the proposed algorithms in [11, 12], the bandwidth efficiency is also reduced. In our

previous work [13], we proposed a new blind estimation algorithm which yields high bandwidth efficiency and high accuracy based on the minimum output variance (MOV). In [13], the performance of the MOV estimator is obtained by simulations. The main objective of this paper is to derive the theoretical mean and variance of the MOV estimator and examine the performance analytically. We also evaluate the performance of the MOV estimator over frequency-selective fading channels and apply the maximal-ratio combining (MRC) technique to improve its performance.

The rest of the paper is organized as follows. In Section 2, the OFDM system model is briefly introduced. In Section 3, the MOV estimator is described and its performance is analyzed over additive white Gaussian noise (AWGN) channels. Numerical results are presented in both AWGN and frequency-selective fading channels in Section 4. Finally, conclusions are drawn in Section 5.

2. OFDM SYSTEMS

OFDM is a form of mutlicarrier modulation and consists of a number of narrowband orthogonal subcarriers transmitted in a synchronous manner. The mth OFDM data block to be transmitted can be defined as $\mathbf{s}(m) = [s_0(m), s_1(m), \ldots, s_{N-1}(m)]^T$, where N is the number of subcarriers. The OFDM signals can be formulated by inverse discrete Fourier transform (IDFT). Using the matrix representation, the mth block of the modulated signal is

$$\mathbf{x}(m) = [x_0(m), x_1(m), \ldots, x_{N-1}(m)]^T = \mathbf{W}\mathbf{s}(m), \tag{1}$$

where $\mathbf{W}$ is the IDFT matrix given by

$$\mathbf{W} = \frac{1}{\sqrt{N}} \begin{bmatrix} 1 & 1 & \cdots & 1 \\ 1 & e^{j\omega} & \cdots & e^{j(N-1)\omega} \\ \vdots & \vdots & \ddots & \vdots \\ 1 & e^{j(N-1)\omega} & \cdots & e^{j(N-1)\times(N-1)\omega} \end{bmatrix}_{N\times N} \tag{2}$$

with $\omega = 2\pi/N$. After the IDFT modulation, a cyclic prefix (CP) is inserted and its length is assumed to be longer than the maximum delay spread of the channel to avoid intersymbol interference (ISI). The resultant baseband signal is upconverted to the radio frequency (RF) and transmitted over a multipath fading channel. At the receiver, the signal is downconverted and demodulated using discrete Fourier transform (DFT) to recover the desired signal. In the absence of CFO, the received signal is given by

$$\mathbf{y}(m) = \mathbf{W}\mathbf{H}\mathbf{s}(m) + \mathbf{n}(m), \tag{3}$$

where

$$\mathbf{H} = \operatorname{diag}\left(H_0(m), H_1(m), \ldots, H_{N-1}(m)\right) \tag{4}$$

represents the channel response in the frequency domain. After down-conversion, the carrier frequency offset Δf is incurred because of the mismatch of carrier frequencies between the transmitter and receiver. The received signal, after the removal of the CP, is

$$\mathbf{y}(m) = \mathbf{\Phi}\mathbf{W}\mathbf{H}\mathbf{s}(m) + \mathbf{n}(m), \tag{5}$$

where

$$\mathbf{\Phi} = \operatorname{diag}\left(1, e^{j\phi_0}, \ldots, e^{j(N-1)\phi_0}\right) \tag{6}$$

denotes the CFO matrix. Note that $\phi_0 = 2\pi\Delta f T_s/N$ and T_s is the OFDM block duration.

3. ESTIMATION OF CARRIER FREQUENCY OFFSET

Due to spectra overlapping, OFDM systems are sensitive to CFO. The CFO destroys the orthogonality among subcarriers, results in intercarrier interference (ICI) and causes system performance degradation. To improve the system performance, the CFO must be estimated and compensated before the DFT demodulation.

3.1. Minimum output variance (MOV) estimator

In the presence of CFO, the received signal, after DFT demodulation, is given by

$$\mathbf{d}(m) = \mathbf{W}^H\mathbf{y}(m) = \mathbf{W}^H\mathbf{\Phi}\mathbf{W}\mathbf{H}\mathbf{s}(m) + \mathbf{n}'(m), \tag{7}$$

where $\mathbf{W}^H$ represents the DFT demodulation matrix, $\mathbf{d}(m) = [d_0(m), d_1(m), \ldots, d_{N-1}(m)]^T$ is the recovered signal vector and $\mathbf{n}'(m)$ is the noise term after the DFT operation. Because of the presence of CFO, $\mathbf{W}^H\mathbf{\Phi}\mathbf{W}$ is no longer an identity matrix and the desired signal $\mathbf{s}(m)$ cannot be recovered properly. For the sake of simplicity, the block number m will not be included in the subsequent derivation. The recovered signal on subcarrier k is given by

$$d_k = I_0 s_k + \sum_{l=0, l\neq k}^{N-1} I_{l-k} s_l, \tag{8}$$

where

$$I_n = \frac{\sin(\pi\Delta f T_s)}{N \sin\left((\pi/N)(\Delta f T_s + n)\right)} \cdot \exp\left(j\frac{\pi}{N}\left((N-1)\Delta f T_s - n\right)\right). \tag{9}$$

In (8), I_0 represents the attenuation and phase rotation of the desired signal and I_{l-k} represents the ICI coefficient from other subcarriers. From (8) and (9), it can be seen that the coefficient I_0 of s_k is independent of k. It implies that the desired signals on all subcarriers experience the same degree of attenuation and phase rotation. Note that the ICI term is the addition of many independent random variables and can be approximated as a complex Gaussian random variable with zero mean [15, 16]. Thus, the output of each subcarrier can be considered as a dominant signal embedded in additive white Gaussian noise. To simplify the analysis, the BPSK modulation is employed in the OFDM scheme.

The ICI power is defined as

$$P_{\mathrm{ICI}} \triangleq E\left|\sum_{l=0, l\neq k}^{N-1} I_{l-k} s_l\right|^2 \tag{10}$$

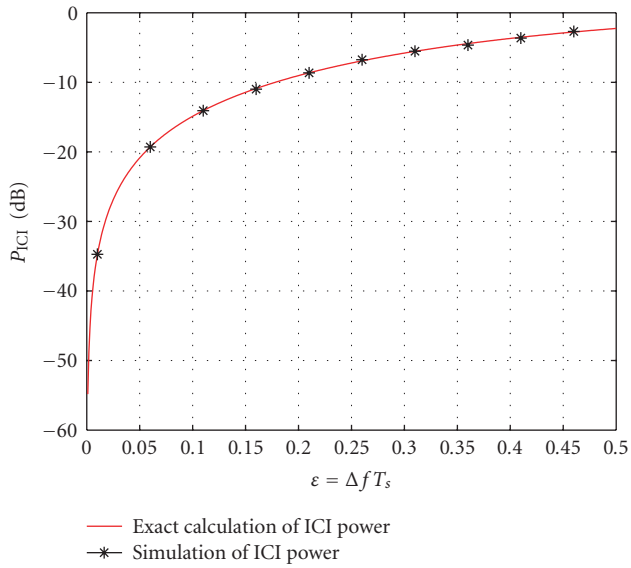

Figure 1: The theoretical and the simulation results of the ICI power.

and P_{ICI} can be obtained as [17]

$$\begin{aligned} P_{\mathrm{ICI}} &= \int_{-1}^{1} (1-|x|)\left(1-e^{j2\pi\epsilon x}\right)dx \\ &= 1-\mathrm{sinc}^2(\epsilon), \end{aligned} \tag{11}$$

where $\epsilon = \Delta f T_s \in (-0.5, 0.5)$ is the CFO normalized to the subcarrier spacing and $\mathrm{sinc}(x) = \sin(\pi x)/(\pi x)$. The theoretical and the simulation results of the ICI power are presented in Figure 1. It is observed that the theoretical curve based on (11) matches the simulation results well.

Since the ICI can be approximated as a Gaussian random variable with zero mean, the variance of the ICI is equal to

$$\sigma^2 = P_{\mathrm{ICI}} = 1-\mathrm{sinc}^2(\epsilon). \tag{12}$$

From (8) and (9), it is clear that the dominant signal on the kth subcarrier is $I_0 s_k$. Hence, the magnitude mean of the dominant signal on the kth subcarrier is

$$m = |I_0 s_k| = \left|\frac{\sin\pi\epsilon}{\pi\epsilon} e^{j\pi\epsilon} s_k\right| = \mathrm{sinc}(\epsilon). \tag{13}$$

Based on the analysis above, the probability density function (PDF) of the output $|d_k|$ can be approximated as Gaussian mixture given by

$$p_{|d_k|}(x) = \left[\frac{1}{\sqrt{2\pi}\sigma} e^{-(x-m)^2/2\sigma^2} + \frac{1}{\sqrt{2\pi}\sigma} e^{-(x+m)^2/2\sigma^2}\right] u(x), \tag{14}$$

where $u(x)$ is the unit step function. Let us consider the expectation and variance of the output $|d_k|$. The expectation of $|d_k|$ is

$$\begin{aligned} E(|d_k|) &= \int_{-\infty}^{\infty} x p_{|d_k|}(x)dx \\ &= \sqrt{\frac{2(1-\mathrm{sinc}^2(\epsilon))}{\pi}} \exp\left\{-\frac{\mathrm{sinc}^2(\epsilon)}{2(1-\mathrm{sinc}^2(\epsilon))}\right\} \\ &\quad + \mathrm{sinc}(\epsilon) - 2\,\mathrm{sinc}(\epsilon) Q\left(\frac{\mathrm{sinc}(\epsilon)}{\sqrt{1-\mathrm{sinc}^2(\epsilon)}}\right), \end{aligned} \tag{15}$$

where

$$Q(x) = \frac{1}{\sqrt{2\pi}} \int_x^{\infty} e^{-t^2/2} dt. \tag{16}$$

The second moment of $|d_k|$ is

$$\begin{aligned} E\left(|d_k|^2\right) &= \int_{-\infty}^{\infty} x^2 p_{|d_k|}(x)dx \\ &= m^2 + \sigma^2 - (m^2+\sigma^2-1) Q\left(\frac{m}{\sigma}\right) = 1. \end{aligned} \tag{17}$$

The variance of $|d_k|$ can be expressed as

$$\mathrm{var}(|d_k|) = E\left(|d_k|^2\right) - E^2(|d_k|). \tag{18}$$

From (15), (17), and (18), it is observed that the expectation and variance of $|d_k|$ are functions of ϵ. Figures 2(a), 2(b), and 2(c) show the expectation, the variance, and the second moment of $|d_k|$ versus the normalized CFO, respectively. From these figures, it is observed that the simulation results match the theoretical results well. The results also show that the variance of $|d_k|$ monotonically increases and the expectation of $|d_k|$ monotonically decreases when the normalized CFO $|\epsilon|$ increases. In other words, the minimum variance and maximum mean are obtained when $\epsilon = 0$. Intuitively, this property can be explained as follows. The CFO does not change the total signal power in one received symbol [14], but the CFO causes the uncertainty of the output. More frequency offset causes more uncertainties and thus, the variance of the output $|d_k|$ increases. This is the principal idea for the CFO estimator proposed in [13].

Based on this property, we have proposed a blind CFO estimator with minimum output variance (MOV) for OFDM systems in [13]. When N is sufficiently large, the expectation of $|d_k|$ is approximately equal to the average value of $|d_k|$ among N subcarriers. From the previous analysis, the average value of $|d_k|$ attains a maximum value if the CFO is properly compensated. Defining

$$\mathbf{\Phi_e} = \mathrm{diag}\left(1, e^{j\phi_e}, \ldots, e^{j(N-1)\phi_e}\right), \tag{19}$$

we search for ϕ_e in the range of $(-\pi/N, \pi/N)$ such that

$$\Lambda(\phi_e) \triangleq \frac{1}{N} \sum_{i=1}^{N} |\mathbf{W}_i^H \mathbf{\Phi}_e^H \mathbf{\Phi W H s}(m)| \tag{20}$$

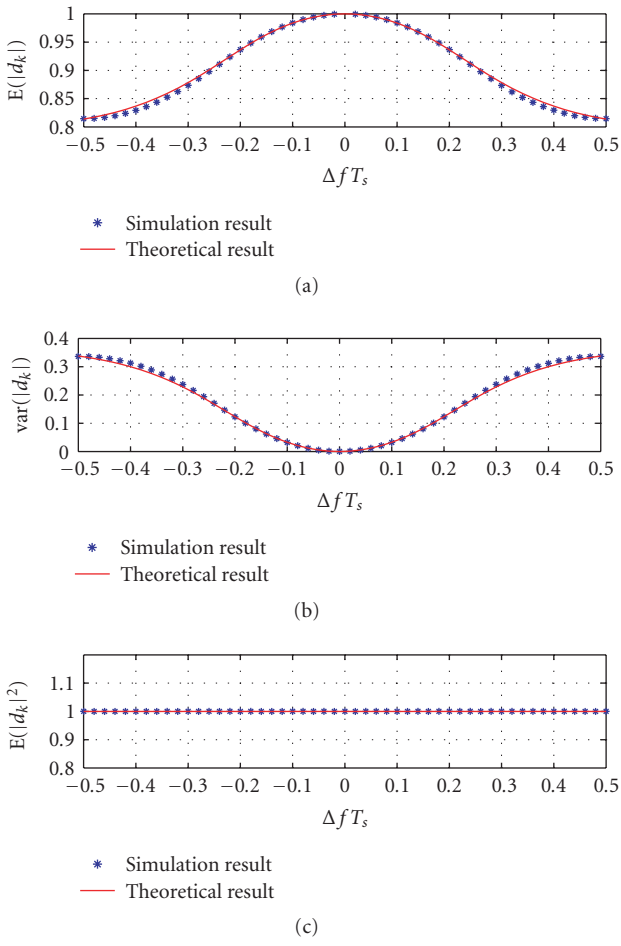

FIGURE 2: (a) Expectation of $|d_k|$ versus ϵ, (b) variance of $|d_k|$ versus ϵ, (c) second moment of $|d_k|$ versus ϵ.

achieves its maximum value for $\mathbf{\Phi}_e = \mathbf{\Phi}$, where $\mathbf{W}_i$ is the ith column of the matrix $\mathbf{W}$. If thermal noise is present, the accuracy of $\boldsymbol{\phi}_\mathbf{e}$ may be improved by searching for the maximal value in (20) with more blocks. Hence, the proposed MOV estimator is to search for one ϕ_e to maximize $\Lambda(\phi_e)$ [13], that is,

$$\hat{\phi}_e = \arg\max_{\phi_e} \frac{1}{MN} \sum_{m=1}^{M} \sum_{i=1}^{N} \left| \mathbf{W}_i^H \mathbf{\Phi}_e^H \mathbf{y}(m) \right|, \tag{21}$$

where $\mathbf{y}(m)$ is defined in (5) and M is the number of blocks used by the MOV estimator. Based on (21), the DFT operation $\mathbf{W}_i^H$ in MOV estimator can be implemented efficiently by means of the fast Fourier transform (FFT) algorithm. Although the above analysis is based on BPSK modulation, it is also applicable to higher-order modulation schemes such as QPSK, 8-QAM, 16-QAM, and 64-QAM, and so forth. Simulations have been conducted to verify that the MOV estimator is applicable to higher-order modulation methods.

3.2. Performance analysis of the MOV estimator

For the MOV estimator, we need to obtain the expected value of $|d_k|$ for each trial value of ϕ_e. The expectation of $|d_k|$ is approximated by the average value of $|d_k|$ among MN outputs, that is,

$$E(|d_k|) = \mu_{\phi_e} \approx \hat{\mu}_{\phi_e} = (1/MN) \sum_{m=1}^{M} \sum_{i=1}^{N} \left| \mathbf{W}_i^H \mathbf{\Phi}_e^H \mathbf{y}(m) \right|. \tag{22}$$

When $|d_k|$ is embedded in AWGN, the accuracy of this approximation is affected and the difference between the expected value and the approximated average value is the major contribution to the error variance of the MOV estimator. It is known that $\hat{\mu}_{\phi_e}$ follows the Gaussian distribution with mean μ_{ϕ_e} and variance σ_w^2/MN [18], where σ_w^2 represents the variance of AWGN noise. Thus, it has a probability that $\hat{\mu}_{\phi_e}$ (for $\phi_e \neq \phi_0$) is greater than the theoretical maximum mean value $\hat{\mu}_{\phi_0}$. When this happens, the estimation accuracy is affected. Equivalently, the analysis can be addressed as follows. Suppose that we have K trial values of ϕ_e among the estimation range and we obtain the average output for each trial value independently. For the kth trial value, the average output is $\hat{\mu}_k = \mu_k + n_k$, where n_k denotes the noise term with zero mean and variance σ_w^2/MN. The probability that $\hat{\mu}_k$ becomes the largest can be expressed as

$$\begin{aligned} &\Pr\left(\hat{\mu}_k = \max\left(\hat{\mu}_1, \ldots, \hat{\mu}_K\right)\right) \\ &\quad = \Pr\left(\hat{\mu}_k > \hat{\mu}_1, \hat{\mu}_k > \hat{\mu}_2, \ldots, \hat{\mu}_k > \hat{\mu}_K\right) \\ &\quad = \Pr\left(\mu_k + n_k > \mu_1 + n_1, \ldots, \mu_k + n_k > \mu_K + n_K\right). \end{aligned} \tag{23}$$

Note that $n_1, n_2, \ldots, n_K$ are independent noise. For a given n_k, the conditional probability can be expressed as

$$\begin{aligned} &\Pr\left(\hat{\mu}_k = \max\left(\hat{\mu}_1, \ldots, \hat{\mu}_K\right) \mid n_k\right) \\ &\quad = \Pr\left(n_1 < \mu_k - \mu_1 + n_k, \ldots, n_K < \mu_k - \mu_K + n_k\right) \\ &\quad = \Pr\left(n_1 < \mu_k - \mu_1 + n_k\right) \\ &\qquad \times \cdots \times \Pr\left(n_K < \mu_k - \mu_K + n_k\right) \\ &\quad = \left(1 - Q\left(\frac{\mu_k - \mu_1 + n_k}{\sqrt{2\sigma_w^2/MN}}\right)\right) \\ &\qquad \times \cdots \times \left(1 - Q\left(\frac{\mu_k - \mu_K + n_k}{\sqrt{2\sigma_w^2/MN}}\right)\right). \end{aligned} \tag{24}$$

Thus, the probability that $\hat{\mu}_k$ becomes the largest is obtained as

$$\begin{aligned} &\Pr\left(\hat{\mu}_k = \max\left(\hat{\mu}_1, \ldots, \hat{\mu}_K\right)\right) \\ &\quad = \int_{-\infty}^{\infty} \Pr\left(\hat{\mu}_k \mid n_k\right) p_{n_k}(x)\, dx, \quad k = 1, 2, \ldots, K, \end{aligned} \tag{25}$$

where $p_{n_k}(x)$ denotes the Gaussian PDF of n_k given by

$$p_{n_k}(x) = \frac{1}{\sqrt{2\pi\sigma_w^2/MN}} \exp\left\{-\frac{x^2}{2\sigma_w^2/MN}\right\}. \tag{26}$$

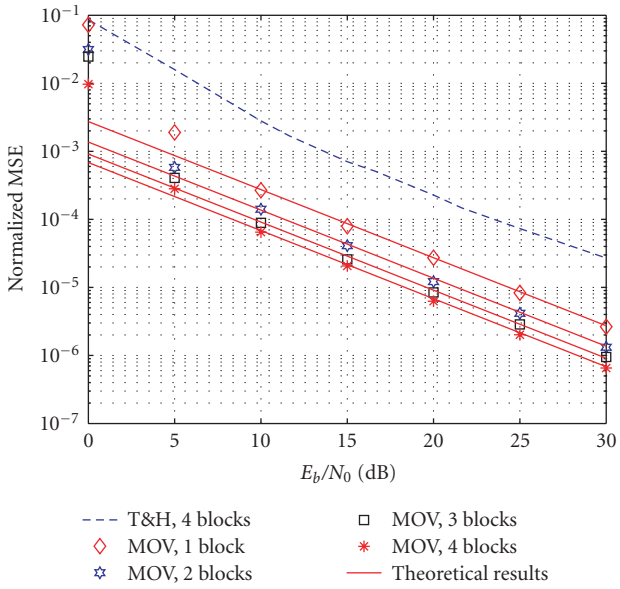

Figure 3: Normalized MSE of the proposed MOV estimator versus E_b/N_0 with various number of OFDM blocks over AWGN channels.

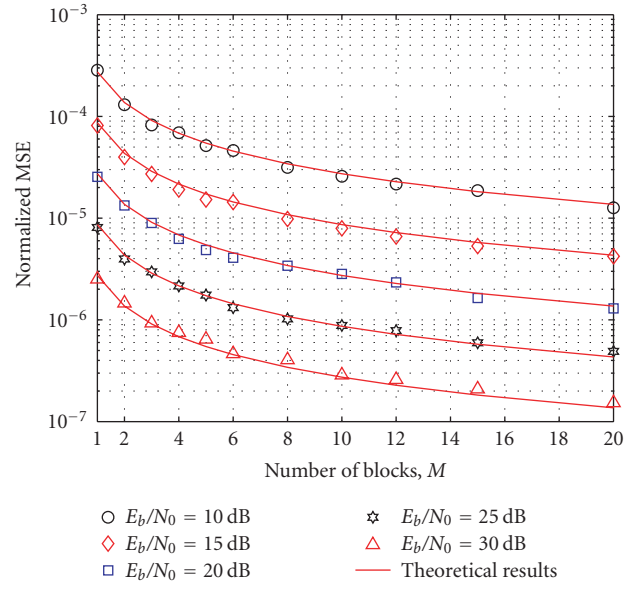

Figure 4: Normalized MSE of the proposed MOV estimator versus number of blocks over AWGN channels.

When all the K probabilities in (25) are obtained, the mean and variance of the estimated offset can be obtained accordingly. Here, the variance represents the mean-square error (MSE) of the MOV estimator. The MSE results will be validated in the next section.

4. NUMERICAL RESULTS AND ANALYSIS

In this section, numerical results are presented to illustrate the performance of the proposed MOV estimator in OFDM systems. In particular, $N = 64$ subcarriers are used. The performance of the proposed MOV estimator is examined by the normalized MSE defined as

$$\text{MSE} = E\left[\frac{|\hat{\phi}_e - \phi_0|^2}{(2\pi/N)^2}\right] \approx \frac{1}{P}\sum_{p=1}^{P}\frac{|\hat{\phi}_{e_p} - \phi_0|^2}{(2\pi/N)^2}, \quad (27)$$

where $\hat{\phi}_e$ is the estimate of ϕ_0 and P is the number of Monte Carlo runs. Simulations are conducted in both AWGN and frequency-selective fading channels.

4.1. Performance over AWGN channels

Figure 3 shows the normalized MSE of the proposed MOV estimator over an AWGN channel. From the simulation results, it is observed that the normalized MSE decreases as E_b/N_0 increases. With more OFDM blocks, the accuracy of the proposed MOV estimator is in general improved. The approximated MSE values are the corresponding solid lines in Figure 3. The simulation results match the theoretical results well at high E_b/N_0, that is, $E_b/N_0 > 10$ dB. The performance curve of the T&H estimator [12] is also included for comparison, where the number of subcarriers is $N = 64$, the number of virtual carriers is $L = 20$, and the number of blocks for estimation is $M = 4$. For the value of MSE $= 10^{-3}$, the proposed MOV algorithm outperforms the T&H algorithm by more than 6 dB in E_b/N_0. The reason for the significant improvement is that the proposed MOV estimator takes the average of the magnitude output and is robust to noise, but the orthogonality property utilized by the T&H estimator is more sensitive to noise. Also, the proposed MOV algorithm can be implemented by fast Fourier transform (FFT) with high efficiency. Thus, the computational complexity of MOV algorithm is generally lower than that of the T&H algorithm.

In Figure 4, we present the MSE results of the proposed MOV algorithm with various numbers of OFDM blocks. From the simulation results, it is observed that the normalized MSE decreases with more OFDM blocks for estimation but using more blocks for estimation increases the complexity of the estimator. Also, the theoretical MSE results match the simulation MSE results well. Note that the normalized MSE is less than 10^{-3} for moderately high E_b/N_0, which makes the degradation caused by the CFO negligible even when only one OFDM block is used for the estimation. Thus, the proposed MOV estimator is also suitable for burst transmission.

4.2. Performance over frequency-selective fading channels

Over frequency-selective fading channels, a 6-path multipath delay profile is assumed. The length of cyclic prefix (CP) is 6 and the maximal delay is not greater than the length of CP to avoid ISI. The MOV estimator takes the average of the output and searches for the maximum mean output. Thus, it is also applicable for frequency-selective fading channels even when

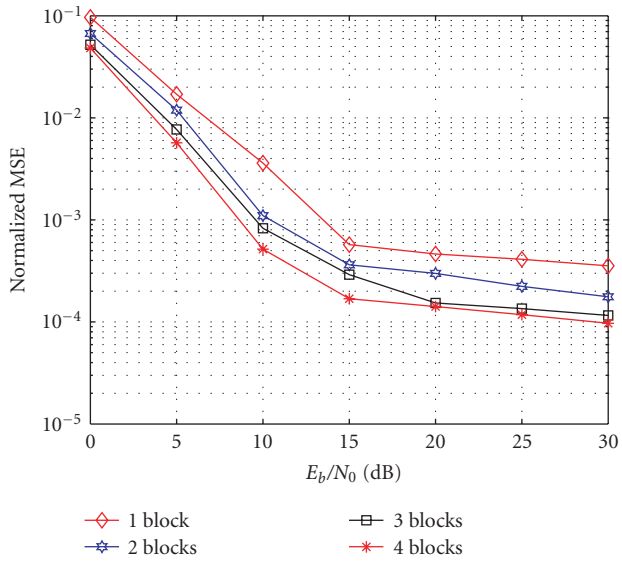

Figure 5: Normalized MSE of the proposed MOV estimator versus E_b/N_0 with various number of OFDM blocks over frequency-selective fading channels.

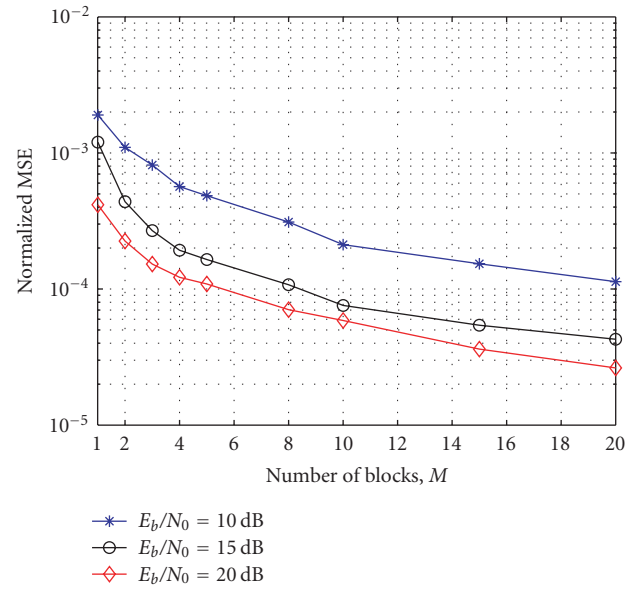

Figure 6: Normalized MSE of the proposed MOV estimator versus number of blocks over frequency-selective fading channels.

the channel information is not available. Figure 5 shows the normalized MSE results over frequency-selective fading channels. From the results, it is observed that the normalized MSE is less than 4×10^{-3} when $E_b/N_0 \geq 10$ dB. The error floor is caused by the channel dispersion. It shows that the algorithm achieves high accuracy with only a few OFDM blocks under moderately high E_b/N_0. Thus, the proposed MOV algorithm is effective and reliable over frequency-selective fading channels.

In Figure 6, the normalized MSE of the proposed MOV algorithm is presented with different number of blocks over frequency-selective fading channels. It is observed that the accuracy is generally improved as the number of blocks increases but the improvement becomes insignificant for large M. Considering the system performance requirement and complexity, the number of estimation blocks M should be properly chosen.

4.3. Performance improvement with MRC technique

The MOV estimator takes the summation of the output over the N subcarriers. It is similar to the combining techniques in multicarrier CDMA (MC-CDMA) [19]. In MC-CDMA systems, many diversity-combining techniques have been applied to improve the system performance, for example, equal-gain combining (EGC) and maximal-ratio combining (MRC). With the MRC technique, the output SNR is maximized [16, 21]. It is interesting to see whether the MRC technique can improve the performance of the proposed MOV estimator over frequency-selective fading channels.

In this subsection, we assume that the channel estimation has been achieved and the channel attenuation and the phase shift on each subcarrier are known to the MOV estimator. Thus, the gain matrix for the MRC is given by [19, 20]

$$\mathbf{G} = \operatorname{diag}\left(H_0^*, \ldots, H_{N-1}^*\right), \tag{28}$$

where H_n is the channel gain on the nth subcarrier in (4) and the superscript $(\cdot)^*$ denotes the complex conjugation. Multiplying with the gain matrix $\mathbf{G}$, the strong signals on subcarriers carry larger weights than weak signals. Thus, the SNR of the output is maximized and the performance of MOV estimator is improved.

According to the channel gain with MRC, the MOV estimator can be rewritten as

$$\begin{aligned}\hat{\phi}_e &= \arg\max_{\phi_e} \Lambda(\phi_e) \\ &= \arg\max_{\phi_e} \frac{1}{MN} \sum_{m=1}^{M} \sum_{i=1}^{N} \left| \mathbf{W}_i^H \boldsymbol{\Phi}_e^H \mathbf{G}\mathbf{y}(m) \right|,\end{aligned} \tag{29}$$

where $\mathbf{G}$ represents the gain matrix for MRC.

The normalized MSE results of the proposed MOV estimator versus E_b/N_0 with MRC technique over frequency-selective fading channels are presented in Figure 7. From the simulation results, it is observed that the normalized MSE significantly decreases with MRC and the performance of the proposed MOV estimator with MRC is even comparable to that of the MOV estimator under the AWGN condition. It is also clear that the error floor is eliminated. This supports the argument that the error floor in Figure 6 is caused by channel dispersion. We also include the performance curve of the T&H estimator [12] for comparison. It is seen that the proposed MOV estimator still outperforms the T&H estimator over the same fading channel conditions.

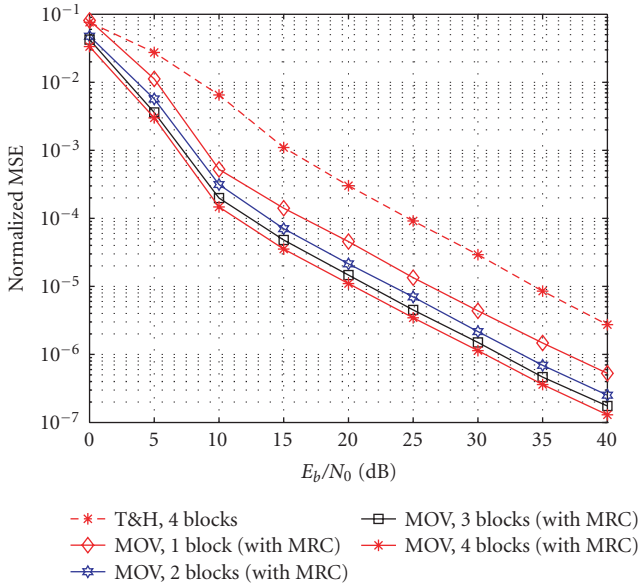

Figure 7: Normalized MSE of the proposed MOV estimator versus E_b/N_0 with MRC technique over frequency-selective fading channels.

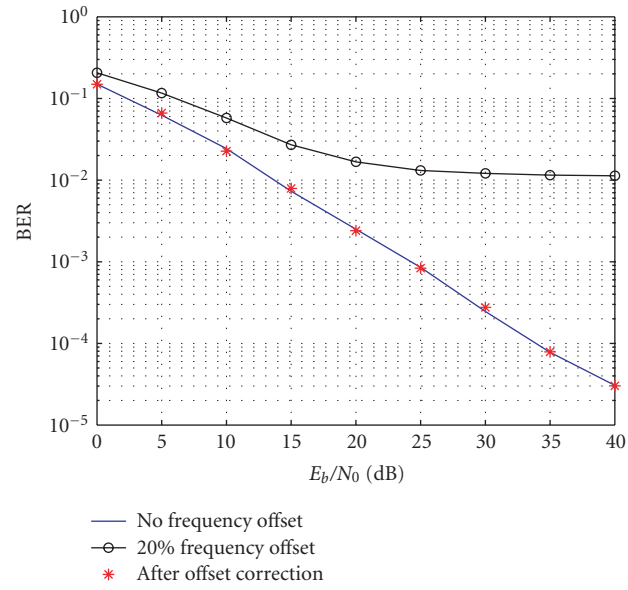

Figure 8: BER versus E_b/N_0 over frequency-selective fading channels.

4.4. Compensation of the CFO

After the CFO estimation is accomplished, frequency offset can be properly compensated and corrected to allow for the data detection. Figure 8 shows the BER performance for three cases, namely, with 20% frequency offset, without frequency offset, and after offset correction over frequency-selective fading channels, respectively. It is observed that the BER has an error floor when there is a 20% frequency offset. The reason for the error floor is that the bit errors are mainly due to the ICI, not due to the noise for high E_b/N_0. The BER, after MOV estimation and correction, is very close to the BER without CFO, which validates that MOV estimator eliminates the effect of CFO effectively.

5. CONCLUSION

In this paper, we have examined the performance of the minimum output variance (MOV) estimator in OFDM systems. The variance and the expectation of the output magnitude have been derived for the MOV estimator. The theoretical MSE of the MOV estimator has been derived and the theoretical MSE results match the simulation results well. From the simulation results, it is observed that the MOV algorithm has high accuracy in both AWGN and frequency-selective fading channels. It has also been shown that the MOV algorithm outperforms the T&H algorithm. The MOV estimator can be implemented by FFT efficiently, which causes the computational complexity of the MOV estimator generally lower than that of the T&H estimator. Furthermore, the maximal-ratio combining (MRC) technique has been applied to the MOV estimator to improve the accuracy over frequency-selective fading channels. Simulation results verify that the MRC technique is effective and significantly improves the accuracy of the MOV estimator over frequency-selective fading channels.

REFERENCES

[1] E. T. Standard, "Radio broadcast systems; digital audio broadcasting (DAB) to mobile, portable, and fixed receivers," Tech. Rep. preETS 300 401, March 1994.

[2] U. Reimers, "DVB-T: the COFDM-based system for terrestrial television," *Electronics & Communications Engineering Journal*, vol. 9, no. 1, pp. 28–32, 1995.

[3] J. Khun-Jush, P. Schramm, U. Wachsmann, and F. Wenger, "Structure and performance of the HIPERLAN/2 physical layer," in *Proceedings of IEEE Vehicular Technology Conference (VTC '99)*, vol. 5, pp. 2667–2671, Amsterdam, The Netherlands, September 1999.

[4] IEEE Std. 802.11a, "Wireless LAN medium access control (MAC) and physical layer (PHY) specifications: High-speed physical layer extension in the 5-GHz band," IEEE, 1999.

[5] *Air Interface for Fixed Broad-Band Wireless Access Systems. Part A: Systems Between 2-11 GHz*, July 2001. IEEE 802.16ab-01/01 Std., Rev. 1.

[6] T. Pollet, M. Van Bladel, and M. Moeneclaey, "BER sensitivity of OFDM systems to carrier frequency offset and Wiener phase noise," *IEEE Transactions on Communications*, vol. 43, no. 2/3/4, pp. 191–193, 1995.

[7] P. H. Moose, "A technique for orthogonal frequency division multiplexing frequency offset correction," *IEEE Transactions on Communications*, vol. 42, no. 10, pp. 2908–2914, 1994.

[8] T. M. Schmidl and D. C. Cox, "Robust frequency and timing synchronization for OFDM," *IEEE Transactions on Communications*, vol. 45, no. 12, pp. 1613–1621, 1997.

[9] J. J. van de Beek, M. Sandell, and P. O. Borjesson, "ML estimation of time and frequency offset in OFDM systems," *IEEE*

Transactions on Signal Processing, vol. 45, no. 7, pp. 1800–1805, 1997.

[10] M. Luise, M. Marselli, and R. Reggiannini, "Low-complexity blind carrier frequency recovery for OFDM signals over frequency-selective radio channels," *IEEE Transactions on Communications*, vol. 50, no. 7, pp. 1182–1188, 2002.

[11] U. Tureli, H. Liu, and D. Zoltowski, "OFDM blind carrier offset estimation: ESPRIT," *IEEE Transactions on Communications*, vol. 48, no. 9, pp. 1459–1461, 2000.

[12] U. Tureli, D. Kivanc, and H. Liu, "Experimental and analytical studies on a high-resolution OFDM carrier frequency offset estimator," *IEEE Transactions on Vehicular Technology*, vol. 50, no. 2, pp. 629–643, 2001.

[13] F. Yang, K. H. Li, and K. C. Teh, "A carrier frequency offset estimator with minimum output variance for OFDM systems," *IEEE Communications Letters*, vol. 8, no. 11, pp. 677–679, 2004.

[14] J. Armstrong, "Analysis of new and existing methods of reducing intercarrier interference due to carrier frequency offset in OFDM," *IEEE Transactions on Communications*, vol. 47, no. 3, pp. 365–369, 1999.

[15] J.-P. Linnartz, "Performance analysis of synchronous MC-CDMA in mobile Rayleigh channel with both delay and Doppler spreads," *IEEE Transactions on Vehicular Technology*, vol. 50, no. 6, pp. 1375–1387, 2001.

[16] W. C. Jakes, *Microwave Mobile Communications*, John Wiley & Sons, New York, NY, USA, 1978, new edition, 1994.

[17] M. Russell and G. L. Stuber, "Interchannel interference analysis of OFDM in a mobile environment," in *Proceedings of IEEE Vehicular Technology Conference (VTC '95)*, vol. 2, pp. 820–824, Chicago, Ill, USA, July 1995.

[18] A. Papoulis and S. U. Pillai, *Probability, Random Variables and Stochastic Processes*, McGraw-Hill, New York, NY, USA, 4th edition, 2002.

[19] N. Yee, J.-P. Linnartz, and G. Fettweis, "Multi-carrier CDMA in indoor wireless radio networks," in *Proceedings the 4th IEEE International Symposium on Personal, Indoor and Mobile Radio Communications (PIMRC '93)*, pp. 109–113, Yokohama, Japan, September 1993.

[20] S. Hara and R. Prasad, "Design and performance of multicarrier CDMA system in frequency-selective Rayleigh fading channels," *IEEE Transactions on Vehicular Technology*, vol. 48, no. 5, pp. 1584–1595, 1999.

[21] J. G. Proakis, *Digital Communications*, McGraw-Hill, New York, NY, USA, 4th edition, 2001.

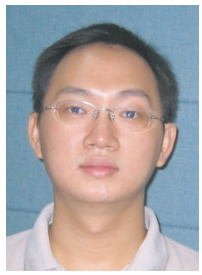

Feng Yang received the B.S. degree in electrical engineering from Huazhong University of Science and Technology, Wuhan, China, in 2002. He is pursuing the Ph.D. degree in electrical engineering at Nanyang Technological University, Singapore. His research interests include OFDM and multicarrier communications, MIMO, UWB, synchronization, and digital signal processing.

Kwok H. Li received the B.S. degree in electronics from the Chinese University of Hong Kong in 1980 and the M.S. and Ph.D. degrees in electrical engineering from the University of California, San Diego, in 1983 and 1989, respectively. Since December 1989, he has been with the Nanyang Technological University, Singapore. He is currently an Associate Professor in the Division of Communication Engineering and has served as the Programme Director of the M.S. programe in communications engineering since 1998. His research interest has centered on the area of digital communication theory with emphasis on spread-spectrum communications, mobile communications, coding, and signal processing. He has published more than 100 papers in journals and conference proceedings. He served as the Chair of IEEE Singapore Communications Chapter from 2000 to 2001. He was also the General Cochair of the 3rd, 4th, and 5th International Conference on Information, Communications, and Signal Processing (ICICS) held in Singapore and Thailand. Presently, he is serving as the Chair of the Chapters Coordination Committee of the IEEE Asia Pacific Board (APB).

Kah C. Teh received the B.E. and Ph.D. degrees in electrical engineering from Nanyang Technological University (NTU), Singapore, in 1995 and 1999, respectively. From December 1998 to July 1999, he was with the Center for Wireless Communications, Singapore, as a Staff R&D Engineer. Since July 1999, he has been with NTU where he is currently an Associate Professor in the Division of Communication Engineering. His research interests are in the areas of signal processing for communications, with special interests in the performance evaluations of interference suppression for spread-spectrum communication systems and multiuser detection in CDMA systems. He received the Excellence in Teaching Award from NTU in the year 2005.